

**GREEN SYNTHESIS OF TiO₂ – Ag
NANOCOMPOSITES FOR SELF-CLEANING AND
ANTIMICROBIAL PROPERTIES ON COTTON
FABRIC**

SUNDERISHWARY S. MUNIANDY

**UNIVERSITI SAINS MALAYSIA
2018**

**GREEN SYNTHESIS OF TiO₂ – Ag
NANOCOMPOSITES FOR SELF-CLEANING AND
ANTIMICROBIAL PROPERTIES ON COTTON
FABRIC**

by

SUNDERISHWARY S. MUNIANDY

**Thesis submitted in fulfilment of the requirements
for the degree of
Master of Science**

May 2018

ACKNOWLEDGEMENT

Foremost, I would like to express my sincere gratitude to the School of Chemical Sciences, Universiti Sains Malaysia (USM) for giving me the opportunity to conduct my research work in fulfillment of my Masters degree. My sincere appreciation to my supervisor Dr. Lee Hooi Ling for the continuous support, patience, motivation, enthusiasm and immense knowledge. Her guidance has helped me in all the time of research and writing of this thesis. I would like to acknowledge the financial support provided by USM Research University Individual Grant (RUI: 1001/PKimia/811265).

My special thanks to my co-supervisor Dr Noor Haida Mohd for her encouragement. I would also like to thank Dr. Sasidharan from INFORMM for his insightful comments, guidance and helping me to understand and interpret the results obtained for the antimicrobial test. Not forgetting, the technical staff from School of Chemical Sciences especially Mr. Sujeyndran, Mr. Zamri, Mr. Ali and Mr. Siva, for the kind assistance and excellent services. Besides, that I would like to thank my lab members and friends especially Vicky, Ruzaina, Loges, Jaga, Johnny, Azia and Mimi for their views and useful discussions. My acknowledgement also goes to respective staff from INFORMM and Institute of Postgraduate Studies (IPS) for their kind assistance and guidance.

Last but not least, my sincere gratitude to my parents, Mr. and Mrs. Muniandy Thanalaxmi, my siblings, VimThinsAgesh, my husband, Dhaarshan Rao and my in-laws, Mr. and Mrs. Sivarao Seetha family for their love, trust and unconditional support throughout my study.

TABLE OF CONTENTS

ACKNOWLEDGEMENT	ii
TABLE OF CONTENTS	iii
LIST OF TABLES	ix
LIST OF FIGURES	xi
LIST OF SCHEMATIC DIAGRAMS	xiv
LIST OF SYMBOLS AND ABBREVIATION	xv
ABSTRAK	xvii
ABSTRACT	xix
CHAPTER 1 INTRODUCTION	1
1.1 Overview	1
1.2 Problems statement	3
1.3 Research objectives	4
1.4 Outline of thesis	4
CHAPTER 2 LITERATURE REVIEW	6
2.1 Solar driven photocatalysis	6
2.2 Concept of a heterogenous photocatalysis	7
2.3 Kinetics of photocatalytic activity	9
2.3.1 Rate constants	9
2.3.2 Langmuir – Hinshelwood kinetics	11
2.4 Metal oxide in photocatalytic activities	13
2.5 Titanium (IV) dioxide (TiO ₂)	14
2.5.1 General	14

2.5.2	Chemical structure and properties of TiO ₂	15
2.6	Modification of TiO ₂ into TiO ₂ nanocomposites	16
2.7	Combination of TiO ₂ with noble metals	18
2.8	Silver (Ag) nanoparticles	19
2.8.1	Properties of AgNPs	19
2.8.2	Concept of antimicrobial activities of AgNPs towards bacteria	20
2.9	Green chemistry principles	21
2.10	Smart textile with self-functioning capabilities	23
CHAPTER 3 MATERIALS AND EXPERIMENTAL METHODS		27
3.1	Materials	27
3.2	Experimental methods	28
3.2.1	Green precipitation synthesis of TiO ₂ nanoparticles	28
3.2.2	Green hydrothermal synthesis of silver nanoparticles	28
3.2.2(a)	Effect of molar ratio of precursor to stabiliser	29
3.2.2(b)	Effect of temperature	29
3.2.2(c)	Effect of reaction time	30
3.2.3	One-pot green hydrothermal synthesis of TiO ₂ -Ag nanocomposites	30
3.2.4	Deposition of TiO ₂ - Ag NCs on fabric	31
3.3	Analytical and characterisation techniques	31
3.3.1	Fourier transform infrared (FTIR)	31
3.3.2	X-Ray diffraction (XRD)	32
3.3.3	Raman spectroscopy	32
3.3.4	UV-Vis spectroscopy	32

3.3.5	Field emission scanning electron microscopy (FESEM)	33
3.3.6	Nitrogen adsorption analysis (NAA)	33
3.3.7	Zeta potential analysis	34
3.3.8	X-ray photoelectron spectroscopy (XPS)	34
3.3.9	Total organic carbon analyser (TOC)	34
3.4	Experimental setup for photocatalytic test	35
3.4.1	Photocatalytic activity of TiO ₂ NPs and TiO ₂ -Ag NCs	35
3.4.2	Control experiments	36
3.4.3	Effect of parameters for photocatalytic test for TiO ₂ NPs	36
3.4.3(a)	Effect of initial pH solution	36
3.4.3(b)	Effect of concentration of precursor	36
3.4.3(c)	Effect of catalyst loading	37
3.4.3(d)	Effect of initial dye concentration	37
3.4.3(e)	Effect of different types of dyes	37
3.4.3(f)	Regeneration and reusability test	37
3.4.4	Effect of parameter for photocatalytic test for TiO ₂ -Ag NCs	38
3.4.4(a)	Effect of precursor (TTIP) loading	38
3.5	Self-cleaning properties of TiO ₂ -Ag NCs deposited cotton fabric	38
3.6	Washing procedure for TiO ₂ -Ag NCs coated cotton fabric	38
3.7	Antimicrobial test for AgNPs, TiO ₂ -Ag NCs and cotton fabric	39
3.8	Experimental Approach	40
CHAPTER 4 RESULT AND DISCUSSION: GREEN SYNTHESIS OF TiO₂ NANOPARTICLES AND THEIR PHOTOCATALYTIC ACTIVITIES		42
4.1	Introduction	42

4.2	Characterisations of synthesised TiO ₂ NPs	42
4.2.1	Fourier transform infrared (FTIR)	42
4.2.2	X-Ray diffraction (XRD) analysis	45
4.2.3	Raman spectroscopy	47
4.2.4	UV-Visible diffuse reflectance spectroscopy (UV-Vis DRS)	48
4.2.5	Field emission scanning electron microscopy (FESEM)	51
4.2.6	Possible formation mechanism of mesoporous TiO ₂	55
4.2.7	Nitrogen adsorption analysis (NAA)	57
4.2.8	Zeta potential analysis	61
4.2.9	X-ray photoelectron spectroscopy (XPS)	64
4.3	Photocatalytic activity and kinetic studies of TiO ₂ NPs	68
4.3.1	Control experiments	68
4.3.2	Effect of concentration of precursor and initial solution pH	69
4.3.3	Effect of catalyst dosage	73
4.3.4	Effect of initial dye concentration	76
4.3.5	Effect of type of dyes	78
4.3.6	Regeneration and reusability of TiO ₂ NPs	81
4.3.7	Physical properties of TiO ₂ NPs after reusability test	82
4.4	Summary	85
CHAPTER 5 RESULT AND DISCUSSION: GREEN SYNTHESIS OF Ag NANOPARTICLES AND THEIR ANTIMICROBIAL ACTIVITIES		86
5.1	Introduction	86
5.2	Characterisation of synthesised AgNPs	86
5.2.1	UV-Vis spectroscopy	86

5.2.1(a)	Effect of molar ratio (AgNO ₃ :PVP) on the formation of AgNPs	86
5.2.1(b)	Effect of reaction time on the formation of AgNPs	88
5.2.1(c)	Effect of temperature on the formation of AgNPs	89
5.2.2	X-Ray diffraction (XRD) analysis	90
5.2.3	Field emission scanning electron microscopy (FESEM)	92
5.2.3(a)	Effect of molar ratio (AgNO ₃ :PVP) on the formation of AgNPs	92
5.2.3(b)	Effect of reaction time on the formation of AgNPs	94
5.2.3(c)	Effect of temperature on the morphology of AgNPs	96
5.3	Possible formation mechanism of AgNPs	97
5.4	Antimicrobial activities of AgNPs	98
5.5	Summary	100

CHAPTER 6 RESULT AND DISCUSSION: SYNTHESIS OF TiO₂ – Ag NANOCOMPOSITES USING GREEN CHEMISTRY APPROACHES FOR THE APPLICATION OF SELF – CLEANING AND ANTIMICROBIAL PROPERTIES ON COTTON FABRIC 102

6.1	Introduction	102
6.2	Characterisation of as – synthesised TiO ₂ –Ag NCs	103
6.2.1	X-Ray diffraction (XRD)	103
6.2.2	Raman spectroscopy analysis	105
6.2.3	Field emission scanning electron microscopy (FESEM)	108
6.2.4	Nitrogen adsorption analysis (NAA)	111
6.2.5	Zeta potential analysis	115
6.2.6	X-ray photoelectron spectroscopy (XPS)	116
6.3	Characterisation of fabric deposited with TiO ₂ –Ag NCs	119

6.4	Photocatalytic activities and kinetic studies of TiO ₂ -Ag NCs	121
6.5	Antimicrobial activities of TiO ₂ -Ag NCs	124
6.6	Self-cleaning performance on cotton fabric	126
6.7	Antimicrobial activities of cotton fabric coated with TiO ₂ -Ag NCs	129
6.8	Summary	131
CHAPTER 7 CONCLUSIONS AND FUTURE WORK RECOMMENDATIONS		133
7.1	Conclusions	133
7.2	Recommendation for future studies	134
REFERENCES		136
APPENDICES		
LIST OF PUBLICATIONS AND CONFERENCES		

LIST OF TABLES

		Page
Table 4.1	FTIR functional group and frequency values for as-synthesised TiO ₂ .	44
Table 4.2	Crystallographic parameters calculated by Rietveld refinement for TiO ₂ NPs synthesized under various conditions.	47
Table 4.3	Textural parameters of mesoporous TiO ₂ NPs samples prepared with different concentration of TTIP and pH of initial solution	61
Table 4.4	Comparison of IEP between various TiO ₂ NPs synthesised under different concentration of TTIP and initial solution pH	63
Table 4.5	Textural parameters, isoelectronic point, rate constants and TOC removal for the degradation of MB by mesoporous TiO ₂ NPs samples prepared with different concentration of TTIP and pH of initial solution	70
Table 4.6	Second order kinetic constants, k''^{-1} for the degradation of MB by mesoporous TiO ₂ NPs samples prepared with different concentration of TTIP and pH of initial solution	71
Table 4.7	Langmuir-Hinselwood constants for the photodegradation of MB solution at different catalyst dosage	75
Table 4.8	Langmuir-Hinselwood constants for the photodegradation of MB solution at different initial dye concentration	78
Table 4.9	Langmuir-Hinselwood constants for the photodegradation of different types of dyes.	80
Table 5.1	Average zon of inhibition (ZOI) against <i>E.coli</i> and <i>B.subtilis</i>	99
Table 6.1	Crystallographic parameters for TiO ₂ - Ag NCs synthesised using different TTIP loadings.	105
Table 6.2	Surface area (S _{BET}), average pore size and total volume of TiO ₂ - Ag NCs prepared using various TTIP loading	114
Table 6.3	Comparison of IEP between various TiO ₂ -Ag NCs synthesised with different TTIP loading	116
Table 6.4	Rate constants, k value for the photodegradation of MB solution by TiO ₂ – Ag NCs synthesised using different TTIP loading	124
Table 6.5	Zone of inhibition measurement for synthesised TiO ₂ -Ag NCs using various TTIP loading against <i>E. coli</i> and <i>B. Subtilis</i>	126

Table 6.6	Self-cleaning property of blank cotton fabric and TiO ₂ -Ag NCs coated fabric at different intervals of sunlight irradiation	128
Table 6.7	Antimicrobial activity (zone of inhibition) of cotton fabric coated with succinic acid, SHP and TiO ₂ -Ag NCs after washing treatments.	131

LIST OF FIGURES

		Page
Figure 2.1	Schematic illustration of photocatalytic mechanism of activated semiconductor photocatalyst	8
Figure 2.2	Bulk crystalline structures of the (a) anatase, (b) brookite and (c) rutile type TiO ₂	15
Figure 2.3	The Twelve Principle of Green Chemistry	23
Figure 4.1	FTIR spectra for (a) soluble starch, (b) uncalcined synthesised TiO ₂ NPs, (c) calcined synthesised TiO ₂ NPs, (d) purchased pure anatase	43
Figure 4.2	X-Ray diffractograms of TiO ₂ NPs synthesized under different concentration of TTIP and initial solution pH	46
Figure 4.3	Raman spectra of calcined and uncalcined TiO ₂ NPs synthesised using 0.01 mol TTIP under basic condition	48
Figure 4.4	(a) Bandgap of TiO ₂ NPs synthesised using various concentration of TTIP and initial pH solution (b) compared bandgap spectra of synthesised sample and pure anatase	50
Figure 4.5	FESEM micrographs (100 000 ×) of the TiO ₂ NPs synthesised using (a) uncalcined TiO ₂ , (b) 0.01 mol TTIP, pH 5, (c) 0.01 mol TTIP, pH 7, (d) 0.01 mol TTIP, pH 9, (e) 0.07 mol TTIP pH 9, (f) pore channels of TiO ₂ NPs (10 000 ×) and (g) wall of mesoporous TiO ₂ NPs (50 000 ×)	55
Figure 4.6	Figure 4.6: Full N ₂ isotherms of TiO ₂ NPs synthesized under different (a) initial solution pH, (b) concentration of TTIP, pore size distribution of TiO ₂ NPs synthesised under different initial solution pH and concentration of TTIP (c) in the range 1-100 nm (d) in the range 1nm-15 nm	60
Figure 4.7	Plot of zeta potential versus pH for TiO ₂ NPs synthesised under different (a) pH of initial solution (b) concentration of TTIP	62
Figure 4.8	High-resolution XPS spectra of (a) Ti 2p, (b) O 1s and (c) C 1s of synthesised TiO ₂ NPs using 0.01 mol TTIP under basic condition	67
Figure 4.9	Figure 4.9: Control experiments for the photocatalytic degradation on 6 mg/L MB solution	68

Figure 4.10	(a) Degradation efficiency and (b) first – order kinetics for TiO ₂ NPs synthesised using different TTIP concentration and initial solution pH	72
Figure 4.11	(a) Plot of MB removal percentage against irradiation time and (b) first – order kinetic plots for degradation MB using different catalyst dosage	74
Figure 4.12	(a) Plot of MB removal percentage against irradiation time and (b) first – order kinetic plots for degradation MB using different initial dye concentration	77
Figure 4.13	(a) Plot of MB removal percentage against irradiation time and (b) first – order kinetic plots for degradation MB using different types of dyes	79
Figure 4.14	Reusability test of synthesised TiO ₂ NPs	81
Figure 4.15	XRD spectra of TiO ₂ NPs after ten recycles	82
Figure 4.16	FESEM micrographs of recycled TiO ₂ NPs (a) pore channels of TiO ₂ NPs, (b) pores on the surface of TiO ₂ after 10 cycles and (c) magnified TiO ₂ NPs.	84
Figure 5.1	UV–Vis spectra of synthesised AgNPs at various molar ratio of AgNO ₃ :PVP under constant temperature (160 °C) and reaction time (24 hr)	88
Figure 5.2	UV–Vis spectra of synthesised AgNPs at different reaction times under constant temperature (160 °C) and molar ratio of AgNO ₃ :PVP (1:5)	89
Figure 5.3	UV–Vis spectra of synthesised AgNPs at different temperatures under constant reaction time (24 hr) and molar ratio of AgNO ₃ :PVP (1:5)	90
Figure 5.4	XRD pattern of the as-synthesised AgNPs using 1:5 AgNO ₃ :PVP at 160 °C for 24 hr.	91
Figure 5.5	FESEM images showing AgNPs synthesised using different molar ratio AgNO ₃ :PVP (a) 1:1, (b) 1:3, (c) 1:5 and (d) 1:7 at 160 °C for 24 hr	93
Figure 5.6	FESEM micrographs of AgNPs synthesised using various reaction time (a) 6 hr, (b) 12 hr, (c) 18 hr and (d) 24 hr using molar ratio AgNO ₃ : PVP (1:5) at 160 °C	95
Figure 5.7	FESEM micrographs of AgNPs synthesised using different temperatures (a) 140 °C and (b) 160 °C	97

Figure 5.8	Partial electron donation of nitrogen to oxygen.	97
Figure 5.9	Reduction and bond between Ag ⁺ ions and PVP molecules.	98
Figure 5.10	Antimicrobial test (disc diffusion assay) of synthesised AgNPs under different molar ratio AgNO ₃ :PVP against (a) <i>E.coli</i> and (b) <i>B.subtilis</i>	100
Figure 6.1	XRD patterns for the 1 mL TTIP, 3 mL TTIP, 5 mL TTIP calcined, 5 mL TTIP uncalcined of synthesised TiO ₂ - Ag NCs and TiO ₂ NPs synthesised using 0.01 mol TTIP under basic condition	104
Figure 6.2	Raman spectra of synthesised TiO ₂ NPs, uncalcined TiO ₂ -Ag NCs, calcined TiO ₂ -Ag NCs in the range 100 cm ⁻¹ - 800 cm ⁻¹ and (b) enlarged image in the range 100 cm ⁻¹ – 300 cm ⁻¹	108
Figure 6.3	FESEM images of the TiO ₂ - Ag NCs synthesised using (a) 1 mL TTIP (b) 3 mL TTIP (c) 5 mL TTIP (d) 5 mL TTIP uncalcined	111
Figure 6.4	(a) N ₂ adsorption/desorption isotherm of TiO ₂ NPs and TiO ₂ -Ag NCs synthesised under different TTIP loading, (b) BJH pore size distribution TiO ₂ NPs and TiO ₂ -Ag NCs	113
Figure 6.5	Plot of zeta potential versus pH for uncalcined, calcined TiO ₂ -Ag NCs synthesised with diferent TTIP loadings and TiO ₂ NPs	116
Figure 6.6	High resolution XPS spectra of (a) Ti 2p, (b) O 1s and (c) Ag 3d of synthesised TiO ₂ – Ag NCs using 5 mL TTIP	118
Figure 6.7	FESEM micrographs of (a) pure cotton fabric (no coatings), (b – c) cotton fabric coated with TiO ₂ -Ag NCs and (d – e) coated cotton fabric after washing	121
Figure 6.8	(a) Degradation efficiency for TiO ₂ – Ag NCs synthesised using various TTIP loading and (b) its first – order kinetics plot	123
Figure 6.9	Ring of inhibition of TiO ₂ -Ag NCs against (a) <i>E. coli</i> and (b) <i>B. Subtilis</i>	125
Figure 6.10	Zone of inhibition for fabric without any coating (A), fabric coated with succinic acid and SPH (B) and fabric coated with succinic acid, SHP and TiO ₂ -Ag NC (C) against: (a) <i>Bacillus subtilis</i> and (b) <i>Esherichia coli</i> .	130

LIST OF SCHEMATIC DIAGRAMS

	Page
Scheme 3.1 Outline of experimental approach	41
Scheme 4.1 Possible formation of pores in TiO ₂ NPs.	57

LIST OF SYMBOLS AND ABBREVIATIONS

Å	Angstrom (= 10^{-10} meters)
Ag	Silver
AgNO ₃	Silver (I) nitrate
BET	Brunauer-Emmet-Teller
BJH	Barret-Joyner-Halenda
eV	Photon energy
FESEM	Field emission scanning electron microscopy
FTIR	Fourier transform infrared
FWHM	Full-width at half maximum
GOF	Goodness of fitness
hr	Hour(s)
IEP	Isoelectronic point
M	Molarity
MB	Methylene blue
min	Minute(s)
mm	Millimeter(s)
MO	Methyl orange
N ₂	Nitrogen
NAA	Nitrogen adsorption analysis
NaH ₂ PO ₄	Sodium hypophosphite
NCs	Nanocomposites
NH ₄ OH	Ammonium hydroxide
nm	Nanometer(s)
NPs	Nanoparticles

NR	Neutral red
ppm	Parts per million
PVP	Polyvinylpyrrolidone
R	Molar ratio
SHP	Sodium hypophosphite
TiO ₂	Titanium (IV) dioxide
TOC	Total organic carbon
TTIP	Titanium (IV) tetraisopropoxide
XRD	X-ray diffraction
XPS	X-ray photoelectron spectroscopy
ZOI	Zon of inhibition

**SINTESIS NANOKOMPOSIT TiO₂ – Ag MENGGUNAKAN
PENDEKATAN KIMIA HIJAU BAGI APLIKASI PEMBERSIHAN SENDIRI
DAN CIRI – CIRI ANTIMIKROB PADA KAIN KAPAS**

ABSTRAK

Pendekatan kimia hijau merupakan pendekatan terbaharu yang dijangka mempunyai implikasi yang luas di semua bidang sains dan teknologi. Walaupun kimia hijau masih lagi di peringkat awal, ia sudah terbukti bahawa ia telah menjadi sebuah aset yang penting dalam meningkatkan prestasi bahan nano serta menarik minat para saintis dari seluruh pelusuk dunia. Nanopartikel titanium dioksida (TiO₂ NP), nanopartikel argentum (AgNP) dan nanokomposit titanium dioksida-argentum (TiO₂- Ag NK) telah berjaya disintesis menggunakan pendekatan kimia hijau. Bahan-bahan yang disintesis telah diuji dalam aktiviti pemangkinan cahaya dan antimikrob yang dipamerkan oleh TiO₂ NP dan AgNP. Mesolintang anatase TiO₂ NP yang terdop sendiri (Ti³⁺) telah disintesis dengan menggunakan kaedah pemendakan mudah pada suhu yang rendah telah menyumbangkan peranan penting dalam aktiviti pemangkinan cahaya. Luas permukaan spesifik TiO₂ NP adalah 87.2 m² g⁻¹ dan purata saiz liang meso adalah 8.7 nm, manakala bagi liang makro adalah 50 hingga 70.2 nm. Kehadiran liang meso dan makro meningkatkan proses fotodegradasi metilena biru (MB) di bawah cahaya matahari. Kesan parameter tindak balas terhadap aktiviti pemangkinan cahaya oleh TiO₂ NP yang disintesis menggunakan 0.01 mol titanium isopropoksida (TTIP) pada pH beralkali telah dikaji dan ia menunjukkan bahawa 0.1 g TiO₂ NP berfungsi dengan lebih baik dalam pewarna kationik (MB). TiO₂ NP yang disintesis mempamerkan ciri – ciri aktiviti pemangkinan cahaya yang tinggi untuk sekurang-kurangnya sepuluh kitaran

penggunaan berpanjangan tanpa kehilangan kecekapannya. Nanopartikel argentum yang seragam (AgNPs) dengan saiz kristal 19.3 nm telah berjaya disintesis dengan menggunakan kaedah hidrotermal yang mudah. Kajian pengoptimuman untuk sintesis AgNP telah ditentukan melalui ujian antimikrob iaitu ujian cakera penyebaran. AgNP yang disintesis dengan menggunakan nisbah molar AgNO_3 : PVP (1:5) pada suhu 160 °C selama 24 jam menunjukkan ciri-ciri antimikrob yang kuat terhadap bakteria Gram negatif (14.3 ± 0.57 mm) daripada bakteria Gram positif (12.3 ± 0.57 mm). Apabila Ag digabungkan dengan TiO_2 , didapati bahawa sifat kedua-dua elemen dalam suatu bahan tunggal (TiO_2 -Ag NK) telah bertambah baik. TiO_2 -Ag NK telah disintesis menggunakan kaedah hidrotermal menggunakan pelbagai muatan asal TiO_2 (TTIP). Kajian telah mengesahkan bahawa saiz Ag dalam TiO_2 – Ag NK yang berkurang secara mendadak sehingga 5 nm telah mendorong kesan sinergi dan secara tidak langsung mendorong aktiviti antimikrob TiO_2 -Ag NK. TiO_2 -Ag NK yang disintesis telah disalut pada kain kapas untuk menghasilkan kain pintar yang mempunyai ciri – ciri pembersihan sendiri dan antimikrob. TiO_2 -Ag NK telah berjaya disalut pada kain dengan bantuan ejen pemautan silang (asid suksinik) dan juga pemangkin (natrium hipofosfit) melalui kaedah hidroterma. Kain kapas yang disalut TiO_2 -Ag NK telah terbukti mempunyai ciri – ciri pembersihan sendiri yang berkesan walaupun selepas empat basuhan.

GREEN SYNTHESIS OF TiO₂ – Ag NANOCOMPOSITES FOR SELF-CLEANING AND ANTIMICROBIAL PROPERTIES ON COTTON FABRIC

ABSTRACT

Green chemistry approach is an emerging interdisciplinary area that is expected to have wide ranging implications in all fields of science and technology. Although green chemistry is still in its infancy, it is already proving to be a useful tool in improving the performance of nanomaterial and generating worldwide interest. Titanium (IV) dioxide nanoparticles (TiO₂ NPs), silver nanoparticles (AgNPs) and titanium dioxide – silver nanocomposites (TiO₂ – NCs) have been successfully synthesised using hydrothermal green chemistry approaches. The synthesised TiO₂ NPs and AgNPs materials were tested in the photocatalytic and antimicrobial studies respectively. A self-doped (Ti³⁺) mesoporous anatase TiO₂ NPs were synthesised using simple precipitation method under low temperature and their significant role in photocatalytic activities was revealed. The surface area of TiO₂ NPs is 87.2 m² g⁻¹ and the average pore size of mesopore is 8.7 nm, meanwhile for macropores are 50 to 70.2 nm. The presence of meso and macropores enhance the photodegradation process of methylene blue (MB) solution under sunlight. The reaction parameters of photocatalytic activities by the TiO₂ NPs synthesised using 0.01 mol of titanium isopropoxide (TTIP) under basic condition showed that 0.1 g of TiO₂ NPs worked effectively in the photodegradation of cationic dye (MB). Synthesised TiO₂ NPs maintained high photocatalytic activities for at least ten cycles of extended usage without losing their efficiency. Uniform silver nanoparticles (AgNPs) with crystallite size 19.3 nm were successfully synthesised using facile

hydrothermal method. Optimisation studies for synthesis of AgNPs were determined using disc diffusion assay for antimicrobial test. AgNPs were synthesised using molar ratio AgNO_3 : PVP (1:5) at 160 °C for 24 hr showed stronger antimicrobial properties against Gram negative (14.3 ± 0.57 mm) bacteria than Gram positive (12.3 ± 0.57 mm) bacteria. When Ag is incorporated with the TiO_2 , it was found that the dual properties of both elements in single material (TiO_2 – Ag NCs) were improved. TiO_2 – Ag NCs were synthesised *via* one- pot hydrothermal method using various loading of TiO_2 precursor (TTIP). Studies confirmed that the size of Ag in TiO_2 NCs reduced drastically to 5 nm which induce the synergy effect and indirectly boost the antimicrobial activities of TiO_2 – Ag NCs. Synthesised TiO_2 – Ag NCs were further coated on cotton fabric in order to produce a smart material with self – cleaning and antimicrobial properties. The TiO_2 – Ag NCs were successfully coated on fabric with the aid of cross – linking agent (succinic acid) and also catalyst (sodium hypophosphite) using hydrothermal method. TiO_2 – Ag NCs coated cotton fabric has been proven to have a promising self – cleaning properties even after four washings.

CHAPTER 1

INTRODUCTION

1.1 Overview

Nanotechnology is still progressive and largely in the "discovery phase" since twenty first century. In general, nanotechnology can be defined as employment of materials at the atomic level by a combination of engineering, chemical, and biological approaches. The modern concept of nanotechnology, which is now considered to be the most widely studied field in science has been attracting a great deal of attention for a variety applications ranging from automotive, biomedical, electrical and so on because of the attractive mechanical, chemical and physical properties offered by the nanoparticles (Suresh, 2013). It is therefore now possible to modify the use of nanostructures in the coating industry to the specific needs of the various applications. In that case, nano-based coatings are widely used today to produce smart materials, for instance, to functionalise surfaces, to provide protection against corrosion and dirt, and to generate attractive designs by special colour effects (Kalangutkar, 2015).

Smart materials obtained through deposition of photoactive nanoparticles on fabrics have gained increasingly more interest on the market due to their multifunctional properties. Typically, new properties can be added on to various fabrics (e.g cotton, polyester, wool, etc.) by incorporating functional agents onto their fibres using chemical or physical procedures. Noble metals and metallic oxide nanoparticles (NPs) are mostly used in developing multifunctional textiles with special properties such as antibacterial activities (against *Escherichia coli*, *Staphylococcus aureus*, and *Klebsiella pneumoniae*) (Samal, Jeyaraman, & Vishwakarma, 2010) and self-cleaning properties on fabric by employing the photocatalytic process on the

fabric with photocatalyst such as titanium dioxide (TiO_2). This smart fabric with enhanced dual functionalities also has enormous potential for improvement of in health industries in order to save the time, energy, material, and subsequently the production cost. Moreover, this technology embraces environmental friendly properties as it efficiently reduces the cleaning efforts and save a significant amount of water and energy (El-Khatib, 2012).

Incorporating noble metals with metal oxides and noble metals have been reported in previous studies (Viana et al., 2013). The use of nanostructured noble metals with antibacterial properties has drawn considerable attention due to their high heat resistance, low decomposability, and long life expectancy. Among noble metals, metallic silver (Ag) has been known as effective antimicrobial agent because Ag is a noble metal that does not corrode during self-cleaning or photocatalytic activity (Yang, 2017). In general, titanium (IV) dioxide (TiO_2) is the most common photocatalyst selected to be incorporated with Ag in order to produce a dual functionalised material, TiO_2 -Ag nanocomposites (TiO_2 -Ag NCs). TiO_2 can be an ideal candidate for integration with Ag since the chemical and physical properties of both metal and metal oxide can be enhanced. TiO_2 , a binary metal oxide with a bandgap of 3.2 eV for anatase has received large attention due to its biological and chemical inertness, cost-effectiveness, low toxicity and ease of preparation in bulk or nanostructured forms.

Abundant conventional methods such as sol-gel technique, chemical precipitation and chemical vapour depositions are applied to synthesize metal oxides (TiO_2 NPs) and noble metals (AgNPs). However, most of the traditional methods employ harmful reagents, long reaction time and required complicated process involving more than one step process as carried by the other reported researchers (Thein, Pung, Aziz, & Itoh, 2015). Therefore, modifying the existing methods for

synthesis of nanomaterials by applying green chemistry principles is considered better as it is eco-friendly, sustainable, and relatively reproducible and the end products are often more stable.

1.2 Problems statement

The production of nanoparticles through expensive conventional physical and chemical methods such as sol-gel, solvothermal and electrochemistry methods resulted in lethal by-products which are hazardous to environment. Although these conventional methods can provide various improvement in nanomaterial for another several hundred years, continuous reliance on them will cause severe problems to our economy and environment. Economic problems are predicted to arise from a steady increase of harmful chemical reagents because of continuous demand but restricted supply. Excessive use of solvents or chemicals and conducting synthesis under high energy for long term may lead to devastation in our ecosystem. Multiple conventional methods has been applied to synthesis TiO_2 and AgNPs in large amounts with well-defined sizes and shapes in a short period of time. However, these techniques use hazardous chemicals, such as organic solvents, reducing agents and stabilisers that are used to prevent unwanted agglomeration of the nanoparticles. Therefore, all these factors can be potentially controlled by synthesis nanomaterials using *via* green chemistry approaches. As a result, the nanoparticles synthesised using green technique have diverse natures and greater colloidal stability. Even though green chemistry has been introduced decades ago, but most of the methods developed to synthesis TiO_2 and AgNPs are two step methods such as two-step sol-gel method or microwave assisted solvothermal method. One potential way to meet these challenges is to synthesis nanoparticle without organic solvents or chemicals, using water as synthesis media and carried out an inexpensive one step reaction.

1.3 Research objectives

The objectives of this research are as follows:

- i. To develop green chemistry techniques in synthesising titanium oxide (TiO₂), silver (Ag) nanoparticles (NPs) and titanium oxide-silver (TiO₂-Ag) nanocomposites (NCs).
- ii. To evaluate the photocatalytic and antimicrobial performance of TiO₂ NPs, AgNPs and TiO₂-Ag NCs under various conditions.
- iii. To deposit TiO₂-Ag NCs on cotton fabrics and compare their antibacterial and photocatalytic properties.

1.4 Outline of the thesis

The thesis consists of seven chapters:

Chapter 1 is the introduction of the thesis. It emphasises on the problem statements, research objectives and outlines of the content.

Chapter 2 is a detailed literature review on some basic knowledge of photocatalysis and antibacterial activities, green chemistry principle and properties of TiO₂ and Ag nanoparticles.

Chapter 3 outlines the general experimental techniques and procedures for synthesising TiO₂ NPs, AgNPs and TiO₂ – Ag NCs using green chemistry approaches. The principles of the instrumental characterisations methods by field emission scanning electron microscope (FESEM), X-ray diffraction (XRD), nitrogen adsorption analysis (NAA), Fourier transform infrared (FTIR) analysis, Zeta potential analysis and X-ray photoelectron spectroscopy (XPS) are briefly discussed.

Chapter 4 summaries the green synthesis and characterisations of TiO₂ NPs under different concentrations of precursor and initial solution pH as reported. Optimisation studies for photocatalytic activity of synthesised TiO₂ NPs were also stated.

Chapter 5 outlines the green synthesis AgNPs *via* hydrothermal route and their antimicrobial studies were investigated and reported. Optimisation parameters for molar ratio of precursors and colloid stabiliser, reaction time and temperature of reaction were described.

Chapter 6 describes the synthesis of TiO₂ – Ag NCs under different concentrations of precursor. The TiO₂ – Ag NCs were then deposited on cotton fabric and tested in both photocatalytic and antimicrobial analyses.

Chapter 7 abstracts a conclusion of the thesis and recommendations for future research.

CHAPTER 2

LITERATURE REVIEW

2.1 Solar-driven photocatalysis

Solar energy is a great and renewable energy source and it is estimated that around 0.01% of the energy of sunlight irradiation is sufficient to supply all the energy that human activities required (Reza Gholipour, Dinh, Béland, & Do, 2015). Most of the solar energy is extensively used in the photochemical process such as photosynthesis. Photochemical process is an economically feasible and environmentally attractive because solar photons can be directly absorbed by catalysts to initiate the reactions. For example, solar photochemical detoxification technologies are extensively applied in the environmental waste management industry by using abundant energy from the sun to degrade the wastes (Kubacka, Fernández-García, & Colón, 2012).

Metal oxide-mediated photocatalysis is expected to be a vital revolution in the employment of solar processes. A metal oxide photocatalyst speeds up the action of light by first absorbing photon and producing electrons and holes. With the abundance of costless solar radiations, a low cost catalyst may be useful for numerous applications (Zyoud et al., 2015). It shows a possible number of promising applications to this environmental technology, because with natural sunlight complete mineralisation of persistent contaminants seems to be the most practical process. Hence, no doubt that detoxifying pollutants by solar-driven photocatalysis using metal oxides as catalysts is full of potential (Robert & Malato, 2002).

2.2 Concept of a heterogenous photocatalysis

The word photocatalysis includes the combination of photochemistry with catalysis. It is a chemical process catalysed by a solid with strong oxidising agent (usually dissolved oxygen) under the energy source which is an electromagnetic field with wavenumbers in the UV visible-infrared range (Robert & Malato, 2002). Photocatalysis may also define as the acceleration of a photoreaction in the presence of a catalyst (Ibhadon & Fitzpatrick, 2013). Photocatalysis generally can be divided into two systems: heterogeneous and homogeneous photocatalysis. Heterogeneous system involve different state of photocatalyst slurries for catalysis, whereas homogeneous photocatalysis is used in a single-phase system (Kubacka et al., 2012). Heterogeneous catalysts have numerous benefits compared to other catalytic processes because they avoid formation of inorganic salts and the recovery of photocatalyst is inexpensive. Heterogeneous photocatalysts are also safe to handle, easy to store and have long life time (Atalay & Ersöz, 2016).

As photocatalyst, the metal oxides must consist of the following properties: (i) capable to absorb visible and/or UV light, (ii) chemically and biologically inert and photo stable, (iii) inexpensive and (iv) non-hazardous (Kubacka et al., 2012). In this case, photo stable means metal oxide which is resistant to change under the influence of radiant energy, especially light. Besides, a semiconductor is different from insulator because semiconductors possess an empty energy region in between highest occupied energy band (valance band (VB)), and the lowest unoccupied band (conduction band (CB)). The empty energy region between the VB and CB is called bandgap (Nyankson et al., 2013).

Generally, photocatalytic activity on semiconductors consists of five basic steps; (1) reactants diffused to the surface of semiconductor, (2) adsorption of reactants onto the surface of solid, (3) reaction on the surface of semiconductor, (4) desorption of products from the surface of the semiconductor and (5) diffusion of products from the surface of the semiconductor (Ibhadon & Fitzpatrick, 2013). The initial process for heterogeneous photocatalysis of organic and inorganic compounds by semiconductors initiates with the absorption of photons with energy equivalent to or greater than the bandgap of the semiconductor. This produces electron-hole (e^-/h^+) pairs which leads to the redox reaction on the surface of semiconductor (Figure 2.1).

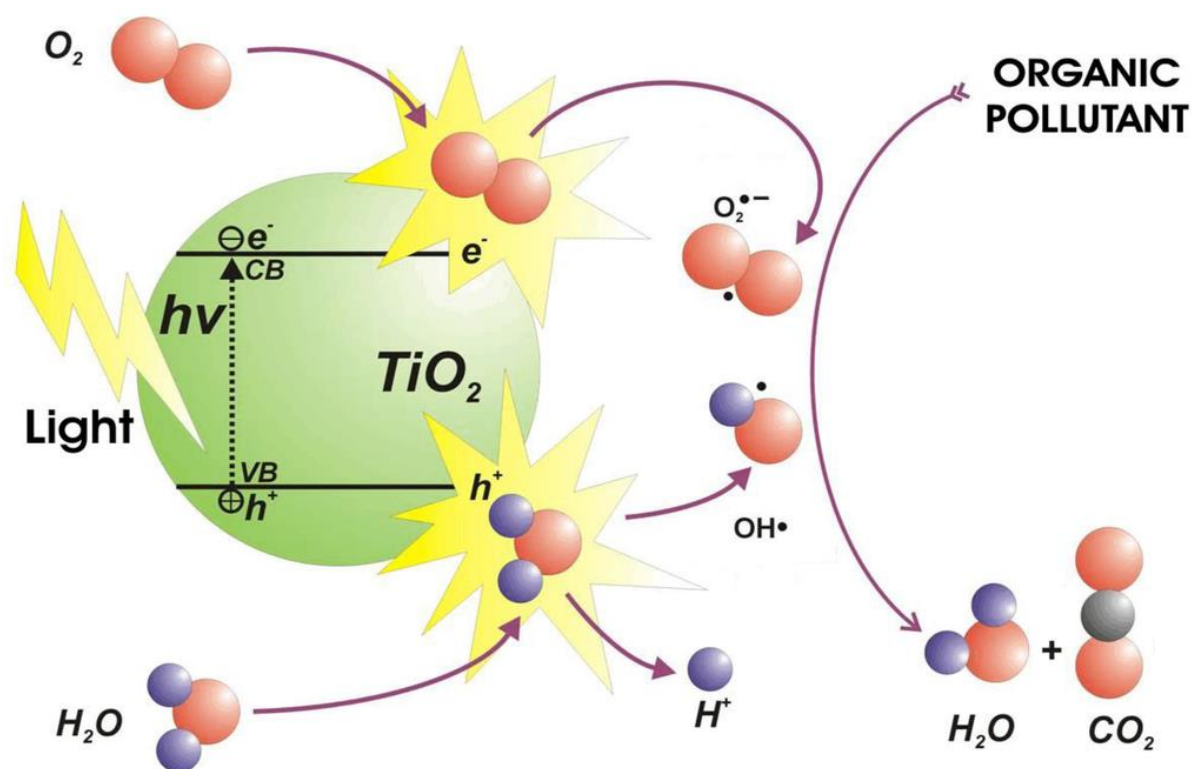


Figure 2.1: Schematic illustration of photocatalytic mechanism of activated semiconductor photocatalyst (Ibhadon & Fitzpatrick, 2013).

Participation of excited electron and the hole in redox reactions with water, hydroxide ion (OH^-), oxygen and organic compounds leading to mineralisation of the pollutant into H_2O and CO_2 . It is also observed that in the absence of H_2O ,

heterogeneous photocatalytic activity could not occur because hydroxyl radicals cannot be created. Subsequently, oxidation of water or OH^- by the hole produces the hydroxyl radical ($\bullet\text{OH}$), a powerful oxidant. $\bullet\text{OH}$ radicals, which are known as the most main radicals are form in semiconductor photocatalysis and they are able to attack the pollutants rapidly on the semiconductor surface. Reduction of adsorbed oxygen to oxygen radicals is a substantial reaction in the conduction band and this stops the electron from recombining with the hole. Hence, the oxygen radicals are accumulated at the conduction bands which can also contribute in degrading waste product in solution (Pelaez et al., 2012). This heterogeneous photocatalytic property of semiconductors provides its self-cleaning property and potentially used in environmental cleaning.

2.3 Kinetics of photocatalytic activity

2.3.1 Rate constants

Chemical kinetics are related with reaction rate and are concerned with both disappearance and appearance of chemical substances. In chemical equilibrium, the reactants and the products are in dynamic state of balance. Generally, for photocatalysis they deal with two types of chemical kinetics; first-order kinetics and Langmuir-Hinshelwood kinetics (Gaya, 2014).

Rate constants, k , are precise for a specific reaction at certain temperatures. The activation energy, E_a , of a reaction is calculated using the temperature dependence rate constants. Subsequently, rate constants are commonly given in a general form as a function of T (the absolute temperature). Thus, if environmental temperatures and reactant concentrations are known, the rates of reactions under various conditions can be evaluated. The units associated with a rate constant depend on the molecularity

(order) of the reaction. This can be proven by rearranging the differential rate equation to isolate k (Wang et al., 2010).

Integrated law for first-order processes:

$$r = \frac{-d[A]}{dt} = k[A] \quad (2.1)$$

$$\ln \frac{[A]_t}{[A]_0} = -kt \quad (2.2)$$

For second-order processes:

$$r = \frac{-d[A]}{dt} = k[A]^2 \quad (2.3)$$

$$-\frac{1}{[A]_t} + \frac{1}{[A]_0} = -kt \quad (2.4)$$

However, first-order kinetics is generally employed for reactions proceeding in homogeneous solution or gaseous phase. The rate of a monomolecular reaction obeys a first-order rate expression that is explained by that proportion (number) of molecules having kinetic energy larger than the activation energy is estimated only by temperature of the reaction. Basically, the first-order kinetics has often been used for discussion of time courses of photocatalytic reactions, meanwhile (pseudo) first-order model is extensively used to determine the adsorption capacity of catalyst in which the experiment for kinetic studies are carried out in dark condition (Vezzoli, 2012; Ayanda, Adeyi, Durojaiye, & Olafisoye, 2012). When an adsorption of products on catalyst was considered, a modified pseudo first-order rate expression is used.

Adsorption capacity at equilibrium needs to be calculated before continuing to pseudo-first-order rate expression:

$$q_e = \frac{(C_0 - C_e)V}{m} \quad (2.5)$$

Where C_0 is the initial dye concentration (mg L^{-1}), C_e is the dye concentration at equilibrium (mg L^{-1}), V is the volume of dye solution used (L) and m is the mass of the catalyst used (mg). The integrated pseudo-first-order model is generally expressed as follows:

$$\log(q_e - q_t) = \log q_e - \frac{k_t}{2.303} t \quad (2.6)$$

Where q_e (mg g^{-1}) and q_t (mg g^{-1}) are adsorption capacity at equilibrium and time t , respectively, while k_t (min^{-1}) is the pseudo-first-order rate constant.

On the other hand, kinetics of reactions occurring on a solid catalyst or photocatalyst surface, are different because monomolecular reaction cannot proceed on the solid surface. Thus for heterogenous catalysis Langmuir-Hinshelwood type of mechanism in the lower concentration region is more appropriate.

2.3.2 Langmuir-Hinshelwood kinetics

In many cases, the Langmuir-Hinshelwood (L-H) kinetic model is widely applied to describe the kinetics of the heterogeneous catalysis system. Most researchers have claimed that a photocatalytic reaction is a surface reaction and it proceeds *via* the L-H mechanism when a linear reciprocal relation is observed between the reaction rate and the concentration of reaction substrate in a solution. A general integrated rate law for L-H model is given below:

$$-\frac{dC}{dt} = k_{LH} \frac{K_L C}{1 + K_L C} \quad (2.7)$$

where, K_L = Langmuir adsorption constant ($L\ mg^{-1}$) and k_{LH} = Langmuir-Hinshelwood reaction rate constant ($mg\ L^{-1}min^{-1}$)

In most photocatalytic kinetic studies it is assumed that the low concentration of substrate, ($mol\ L^{-1}$) $< 10^{-3}$ (Lazar, Varghese, & Nair, 2012; Ferreira, Asenjo, Santamarı, & Mene, 2017), the term K_L becomes < 1 , when the denominator on equation (2.7) is neglected and the equation (2.7) can be reduced to an apparent integrated first order reaction:

$$\ln \frac{C_0}{C_t} = k' t \quad (2.8)$$

However, if $K_L \gg 1$ (at high concentration of substrate) then equation (2.7) becomes a zero order expression (Eng et al., 2013), indicating a broad coverage of the active centers by the organic molecules:

$$\ln \frac{C_0}{C_t} = k'' \quad (2.9)$$

Where, C_t is the concentration of methylene blue (MB) at t time(min), and k' , k'' are the rate constants for L-H first-order and zero-model, respectively.

According to numerous evaluations on L-H kinetic model, the first-order kinetic expression has been proved to be compatible with most of the photocatalytic activities of semiconductors (Joonwichien, Yamasue, Okumura, & Ishihara, 2011). Besides, in order to determine the superiority of new photocatalysts over commercialised photocatalysts in market such as P25 Degussa TiO_2 (Acros Organics, New Jersey, USA), many physicochemical characteristics of the

photocatalysts such as the crystallinity, size, surface defects, specific surface area and aggregation of particles are investigated and compared (Rochkind, Pasternak, & Paz, 2015; Ibhaddon & Fitzpatrick, 2013).

2.4 Metal oxides in photocatalytic activities

Different semiconducting materials with various bandgap energies have been evaluated as photocatalysts in the literatures (Nagaveni, Hegde, Ravishankar, & Subbanna, 2004; Genuino, Huang, Njagi, Stafford, & Suib, 2012). An ideal photocatalyst is expected to have certain advantages such as easy to produce and use, cost effective, photostable, non-hazardous for humans and the environment, efficiently activated by solar light and able to catalyse the chemical reaction proficiently (Kubacka et al., 2012).

The semiconductors such as TiO_2 , ZnO , SrTiO_3 , CeO_2 , WO_3 , Fe_2O_3 and CuO have shown promising redox or charge-transfer processes because of their electronic structures which are characterised by a filled valence band and an empty conduction band. However, most of the reported photocatalysts possess disadvantages. They are not appropriately used in catalysis in aqueous media as they readily undergo photo-corrosion problems upon excitation in solution. ZnO is still unfavourable when compared to TiO_2 because it is readily dissolved in water to produce Zn(OH)_2 on the ZnO particle surface, which deactivates the catalyst after being used for several times. Fe_2O_3 , on the other hand, is well-known for its low cost and narrow bandgap for harnessing solar energy. However the only disadvantage for using Fe_2O_3 is that it suffers from rapid charge recombination and a short charge carrier diffusion length (Ibhaddon & Fitzpatrick, 2013). Meanwhile, SnO_2 and WO_3 possess a conduction band edge at an energy level below the reversible hydrogen potential where these materials

need an aid of an exterior electrical bias to complete the photocatalytic process (Gupta & Tripathi, 2011).

TiO₂ is the most commonly used photocatalyst for degradation of a wide range of pollutants because it fulfills all of the above requirements as well as displaying sufficient conversion values (Kubacka et al., 2012). TiO₂ in its anatase form is effective, photochemically stable, non-toxic in nature and inexpensive. Moreover, due to its strongly oxidised holes and highly redox selective, several novel heterogeneous photocatalytic reactions and self-cleaning properties have been explored extensively for environmental cleanup applications.

2.5 Titanium (IV) dioxide (TiO₂)

2.5.1 General

Titanium dioxide (TiO₂) belongs to the family of transition metal oxides. It is a naturally occurring oxide of Titanium (Ti). The unique properties of TiO₂ is directly connected to its crystal structure which is also related to its processing method (Nyankson et al., 2013). As n-type semiconductor, TiO₂ is photoactive, biologically and chemically inert, resistant to photo and chemical corrosion, low cost, long durability and low toxicity (Vadlapudi & Behara, 2013). Due to its excellent pigmentary properties, high ultraviolet absorption and high thermal stability, TiO₂ is has been used in diverse applications such as electro-ceramics, glass, paints, sunscreen, self-cleaning surfaces, air and water purification, water splitting and photoelectrochemical conversion (Pelaez et al., 2012).

2.5.2 Chemical structures and properties of TiO₂

The unique properties of TiO₂ is directly related to its crystal structure. It is also reported as one of the factors affecting its activity. TiO₂ generally occurs in nature in three crystallographic phases (Figure 2.2):

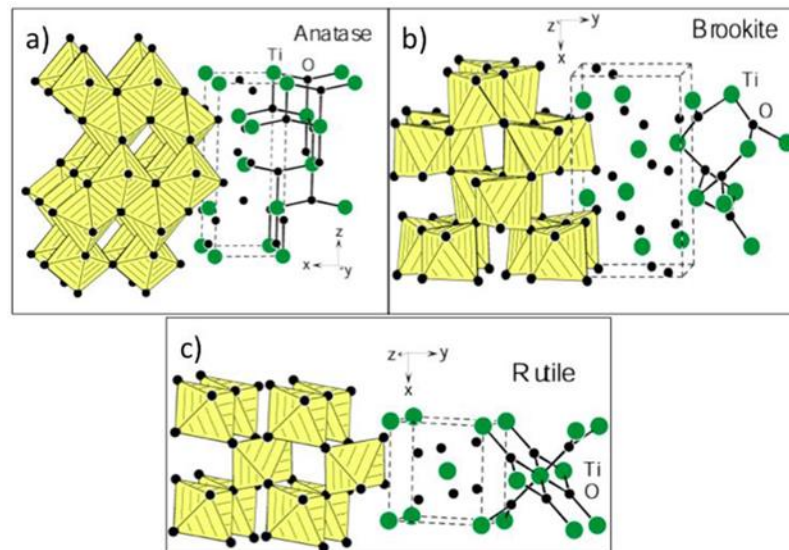


Figure 2.2: Crystalline structures of (a) anatase, (b) brookite and (c) rutile TiO₂ (Reza Gholipour et al., 2015).

- 1) Anatase: It has the distortion of the TiO₆ octahedron and is slightly larger compared to rutile phase. Anatase is made up of corner (vertice) sharing octahedra which form (001) planes resulting in a tetragonal structure.
- 2) Rutile: It is the primary source and the most stable form of TiO₂ at most pressures and temperatures. In rutile, the octahedra share edges at (001) planes to give a tetragonal structure.
- 3) Brookite : It has an orthorhombic crystal system. Its unit cell is composed of 8 formula units of TiO₂ and is formed by edge and corners sharing TiO₆ octahedra.

TiO₂ is a large band semiconductor, with bandgaps of 3.2, 3.0, and ~3.2 eV for the anatase, rutile and brookite phases, respectively. Even though, rutile exhibits the lowest bandgap, the anatase structure is preferred over other polymorphs because of its higher electron mobility and lower density (Kandiel, Robben, Alkaim, & Bahnemann, 2013). Brookite known as the least active phase of TiO₂ due to its more complicated crystalline structure with larger cell volume. It is also the least dense compared to anatase and rutile (Gupta & Tripathi, 2011).

Normally, when anatase and brookite TiO₂ are introduced with temperatures exceeding 600 °C, they will be transformed into more thermodynamically stable rutile which has a very poor photocatalytic activities. The transformation is also influenced by other factors such as synthesis conditions, types of precursors used, impurities, oxygen vacancies and the primary particle size of the anatase phase (Reza Gholipour et al., 2015).

2.6 Modification of TiO₂ into TiO₂ nanocomposites

Nanocomposite is a combination of matrix, in which different materials combine to develop new properties ensuring that one of the materials has size in the range of 1-100 nm. Various researches have been exploited to modify TiO₂ into nanocomposites using numerous approaches to improve the performance TiO₂ nanomaterials and to produce an end product with dual functionalities. Although the use of pure TiO₂ as a UV absorber is possible, it has become clear that this is less feasible for utilising photoelectrochemical properties of TiO₂ alone into the biological applications. Thus, more researches have been dedicated to the construction of nanoscale TiO₂ composite materials (Dastjerdi, Montazer, & Shahsavan, 2010). In addition, there have been great efforts to incorporate additional components including

polymers, transition metals, metal oxides and noble metals to develop the properties of TiO₂ or to provide multi-functioned TiO₂.

Many polymer nanocomposites have been manufactured using polyester, polypropylene, polyethylene, nylon with TiO₂ as fillers to improve the surface area to volume ratio, and to develop system energy and structure of TiO₂ (Chaudhari, 2015). Polymers are also incorporated with TiO₂ to immobilise the TiO₂ powders which improve the reusability efficiency of the photocatalyst. Moreover, instead of using a single semiconductor (TiO₂), uniting the TiO₂ with other semiconductors or metals would lead to the development of a heterojunction structure between them. Besides, coupling collective oscillations of the electrons were found to improve the performance of several devices such as solar cells (Reza Gholipour et al., 2015; Chen & Mao, 2007).

Since TiO₂ is known to have a broader range of applications in healthcare, environmental, cosmetic and food industries, modified TiO₂ with noble metals are considered to be more effective due to different physicochemical properties in comparison to their fine particles. Modified TiO₂ with noble metals are also used significantly in environmental applications like water and air purification, dye removal and solar water splitting. In addition, TiO₂-noble metal composites have also been explored extensively in biomedical applications such as in photodynamic therapy (PDT) for cancer, drug delivery system, cell imaging, biosensors for biological assay, and as endonucleases in genetic engineering (Ghosh & Das, 2015). Thus, the synthesis of numerous nanocomposites of TiO₂ semiconductor with several noble metals will be further discussed in the following section. These composites are considered to have unique dual properties that is yielding the greatest benefits in diverse applications.

2.7 Combination of TiO₂ with noble metals

Several strategies have been employed for modification of TiO₂ nanoparticles. However, incorporation of noble metals to TiO₂ has received the utmost attention compared to polymer/ceramic based nanocomposites because of its hybridisation of two or more materials with distinctive properties. This acts synergistically to develop new functionalities and hence improving their properties. One of the reasons semiconductor NPs coupled to noble metals co-catalyst is to increase the effectiveness of photocatalytic reaction by enhancing the quantum yield of the electron transfer processes. The electron transfer process occurred during the charge separation route in the semiconductor where photogenerated electrons were discharged across the interface and providing a redox pathway with low over-potential. Thus, when the metal nanoparticles are introduced to semiconductor nanoparticles, they able to accept and transport electrons to an acceptor molecules easily (Ibhadon & Fitzpatrick, 2013).

TiO₂ composite systems have been analysed from the starting point of the photocatalysis research field. Fine noble metals that have been investigated are Ag, Pt, Pd and gold Au (Kubacka et al., 2012). Among metal nanomaterials, metallic Ag has been known as effective composite material to be merged with TiO₂ because Ag is a noble metal that does not corrode under photocatalytic conditions. For economical and resourceful use of Ag, composite materials incorporating Ag nanoparticles have been developed and verified in diverse applications.

Generally, TiO and metal incorporated based on two main models which correspond to phase-coupled or coreshell geometries. In addition to the improvement of photocatalysis, composite structures can yield other benefits. For example, addition of Ag noble metal to TiO₂ can yield a product consist of self-cleaning and antimicrobial

properties. Further, composites can be of great use to create highly porous materials, hollow shells and hierarchical structures by templating methods (Dahl, Liu, & Yin, 2014).

2.8 AgNPs

2.8.1 Properties AgNPs

AgNPs material has been studied and exploited in large extent to obtain a complete and organized perspective of AgNPs. In fact, it was reported that nanosilver had a history of approximately 120 years of usage, mainly under the term ‘colloidal silver’ (Yang, 2017). Any noble metals employed in optical detection are usually to obtain the surface plasmon resonance (SPR) effect and Ag shows the highest SPR band intensity than any other NPs like copper and gold. Since Ag NPs show sharper and stronger peaks of plasmon resonance than gold NPs at the equal concentration of particles. This phenomenon proves that the AgNPs have higher plasmon efficiency compared to gold NPs. For this reason Ag NPs show better sensitivity for applications like surface enhanced Raman scattering and localised SPR surface plasmon resonance (Nurani, Saha, Rahman Khan, & Sunny, 2015).

Moreover, nano-sized Ag has distinctive physical, chemical and biological properties compared to their micro-scaled counterparts. AgNPs have unique physico-chemical properties, surface-enhanced Raman scattering, high chemical stability, non-linear optical behaviors and high catalytic activity. These properties induce them to display wide spectrum bactericidal and fungicidal activities (Srikar, Giri, Pal, Mishra, & Upadhyay, 2016) that have made them tremendously popular in a various range of consumer products, including textiles, food, plastics, soaps and pastes. To date, nanosilver technologies have appeared in a variety of manufacturing processes and end products (Tran, Nguyen, & Le, 2013). The following sections will cover the

antimicrobial effects of AgNPs and their mechanisms involved in antimicrobial activity.

2.8.2 Concept of antimicrobial activities of AgNPs towards bacteria

AgNPs have received great attention due to its strong toxicity to a widespread range of microorganisms, including Gram-positive and Gram-negative bacteria. The highest antibacterial activities has been found against *Streptococcus pyogenes*, *Staphylococcus aureus* and *Staphylococcus epidermidis* and moderate sensitivity against *Klebsiella pneumonia* and *Salmonella typhi* (Nurani et al., 2015). The properties such as shape, size, morphology, aggregation level of AgNPs play an important role in the nanoparticles antibacterial activities. Properties of AgNPs normally can be affected by a number of factors such as the type of stabiliser employed and the techniques used for synthesis of nanoparticles (Zewde, Ambaye, Iii, & Dharmara, 2016). For example, many studies claimed that small Ag particles synthesised using numerous techniques have higher antibacterial activities than the big Ag particles because the antibacterial activities are largely depended on the penetrating ability and the surface to volume ratio of particles. (Renaud, Renaud, Sarantopoulos, & Maury, 2010).

Various mechanisms of the inhibitory effect of AgNPs on bacteria have been suggested. The AgNPs show efficient antimicrobial properties compared to other salts due to their extremely large surface area, which provides better contact with microorganisms. Both Gram positive and Gram negative bacteria hold the same mechanism. Generally, antibacterial activities of AgNPs ranging from (a) formation of pits in cell wall, (b) interference of cell membrane and (c) binding of AgNPs with basic residues within the cell components.

AgNPs have high affinity towards phosphorus and sulphur, and hence it exhibits an efficient antibacterial effect. AgNPs react with the sulphur-containing amino acids outside or inside the cell membrane *via* free radical formation by AgNPs and indirectly inhibit the respiratory enzymes of the microorganism. When AgNPs enter the bacterial cell the Ag⁺ ions are released from the AgNPs forming a low molecular weight region in the centre. However, the bacteria conglomerates, protecting the DNA from the Ag⁺ ions. In that case, the AgNPs or Ag⁺ ions attack the respiratory chain, cell division which results the stoppage of DNA replication and finally, leading to cell death of the bacteria. (Rai, Yadav, & Gade, 2009)

2.9 Green chemistry principles

Green Chemistry, which is also named as sustainable chemistry, is defined as the design of chemical products and processes to decrease or remove the use and generation of toxic substances. (Atalay & Ersöz, 2016). This definition and the concept of Green Chemistry were first formulated at the beginning of the 1990s. Green Chemistry is also well-known for its practice of chemical science and manufacturing by taking into account the important rules such as non-polluting and consuming minimum amounts of materials and energy while producing little to no waste materials. It includes novelty, planning and systematic conception too (Malik, Shankar, Malik, Sharma, & Mukherjee, 2014); (Hutchison, 2007). The field of Green Chemistry has revealed how chemists can design next generation products and processes to ensure that they are profitable while being safe to the environment and human health. The design of environmentally benign chemicals and processes are guided by the 12 Principles of Green Chemistry developed by Anastas and Warner summarised (Figure 2.3).

Furthermore, green nanoscience/nanotechnology involves the application of green chemistry principles to the design of nanoscale products, the expansion of nanomaterial production techniques and the application of nanomaterials. It focuses on the discovery of synthesis and production of nanomaterials that eliminate the use of harmful reagents while providing the compulsory volume of pure material in economically practicable manner. It also provides practical designation to ensure the nanomaterials produced are biologically and ecologically safe. Finally, the application of nanomaterials synthesised must take into account where it provides maximum social advantage while reducing the effect on the ecosystem (Anastas & Eghbali, 2010); (Pattanayak, Basak, & Nayak, 2014).

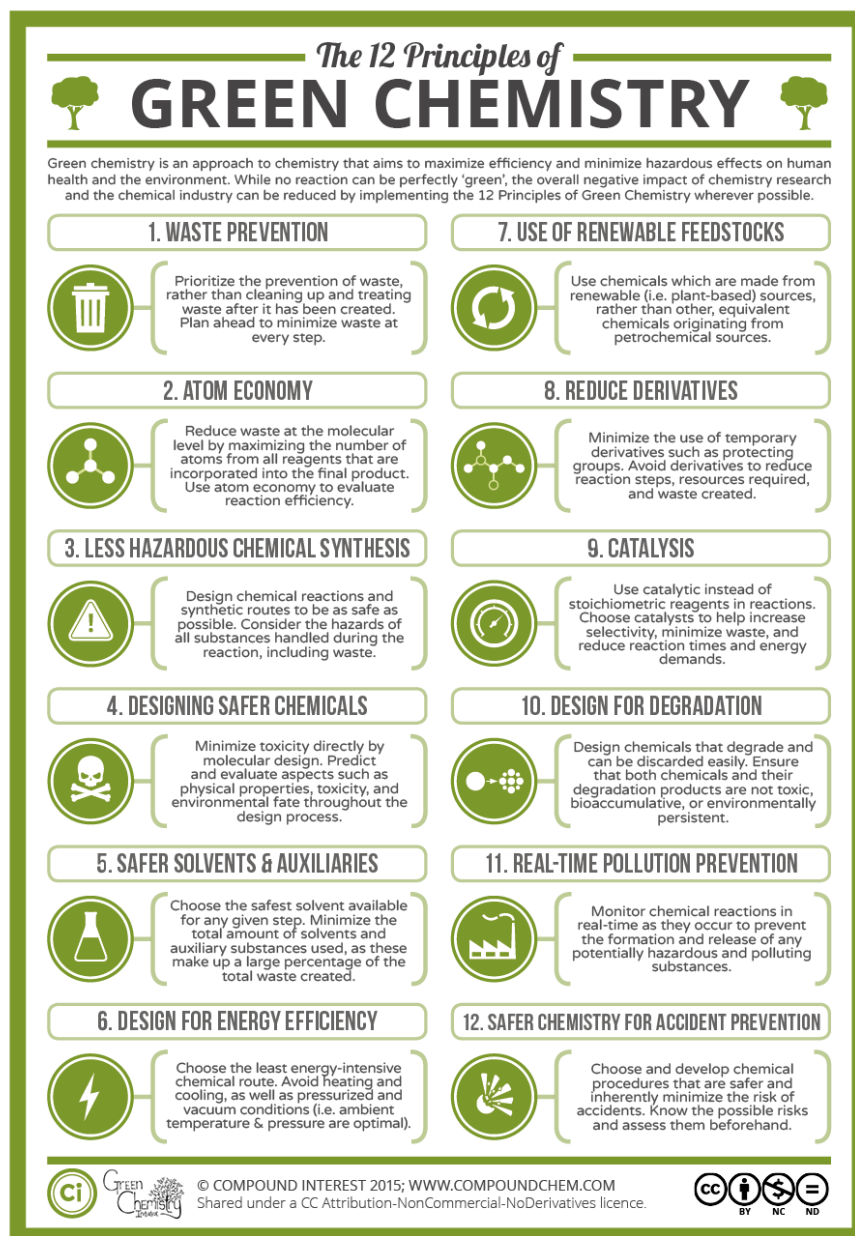


Figure 2.3: The Twelve Principle of Green Chemistry (Source: <http://www.compoundchem.com/2015/09/24/green-chemistry/>)

2.10 Smart textile with self-functioning capabilities

Textile products play an important role in our basic need. They are commonly produced and used in clothing industry. Textiles or fabrics are also vital in other industries such as agricultural industry, transportation, building material and also health industry. Therefore, the technological advances of textiles are improved in order

to meet the need of various industries. Smart textiles, which are textiles with innovative and mechanical applications, can receive and give responses to the external stimuli in order to adapt to the technological changes in surrounding. ‘Self-functioning’ is an ability of a matter to perform a specific process or response automatically towards a corresponding requirement. In latest decades, implementation of smart textile with different 'self-functioning' competencies have been opened up progressively. Self-functional fabrics are widely acknowledged of bringing great benefits to the sustainable growth of society and to stimulate the quality of life as well (Morais, Guedes, & Lopes, 2016)

A fabric with self-cleaning function is known to be capable of decomposing or removing dirt automatically that can reduce human effort, detergents and water required in cleaning. The functions for self-cleaning include dirt and organic substances decomposition, pollutant degradation, deodorisation, anti-mould, and anti-bacteria. In recent years, photocatalytic coating is a popular approach for developing self-cleaning textiles. Photocatalysts, which are able to absorb light energy and decompose the organic matters during the process of photo catalysis, had been utilised for the invention of new self-cleaning textiles. Titanium dioxide (TiO_2), zinc oxide (ZnO) and porphyrins are the significant examples of photocatalysts.

The study of titanium dioxide (TiO_2) coatings on fabric surfaces had been reported in current years. Nano-crystalline TiO_2 finishing on cotton fabrics' surface by dip-pad-dry-cure process had been produced. ‘Self-cleaning’ degradation of the organic materials such as colorant, red wine, coffee stains and bacteria under ultra-violet (UV) irradiation was successfully reported in previous study (Ambika & Sundrarajan, 2014). Although the substantial performance of degrading organic